

Pair-breaking effects induced by 3-MeV proton irradiation in $\text{Ba}_{1-x}\text{K}_x\text{Fe}_2\text{As}_2$ Toshihiro Taen,* Fumiaki Ohtake, Hiroki Akiyama, Hiroshi Inoue, Yue Sun, Sunseng Pyon, and Tsuyoshi Tamegai
Department of Applied Physics, The University of Tokyo, 7-3-1 Hongo, Bunkyo-ku, Tokyo 113-8656, Japan

Hisashi Kitamura

Radiation Measurement Research Section, National Institute of Radiological Sciences, 4-9-1, Anagawa, Inage-ku, Chiba 263-8555, Japan

(Received 8 October 2013; revised manuscript received 14 December 2013; published 30 December 2013)

Pair-breaking effects induced by 3-MeV proton irradiations are examined in underdoped, optimally doped, and overdoped $\text{Ba}_{1-x}\text{K}_x\text{Fe}_2\text{As}_2$ single crystals in terms of suppression of the superconducting critical temperature T_c . The small residual resistivity (RR) in as-grown crystals shows the presence of negligible intrinsic scatterings, which makes this material a model system for studying the effect of artificially introduced scatterings. The RR and T_c change linearly with the proton dose. As in the case of proton irradiation in Co-doped BaFe_2As_2 , we do not detect any low-temperature upturns in resistivity attributable to magnetic scattering or localization. Regardless of K doping levels, the critical value of the normalized scattering rate is much higher than that expected in s_{\pm} -wave superconductors.

DOI: [10.1103/PhysRevB.88.224514](https://doi.org/10.1103/PhysRevB.88.224514)

PACS number(s): 74.70.Xa, 74.62.En, 74.25.fc

I. INTRODUCTION

The superconducting gap structure and the underlying pairing mechanism of iron-based superconductors (IBSs) are under intense debate. Nevertheless, no consensus has been established. At a very early stage, it was claimed that the superconductivity in IBSs was mediated by antiferromagnetic (AFM) spin fluctuations, leading to the so-called s_{\pm} -wave gap structure.^{1,2} Namely, the opposite sign of the order parameter between hole and electron Fermi surfaces (FSs) is realized via interband scatterings between hole and electron FSs. However, another perspective has been proposed that the orbital degrees of freedom play an important role in various physical properties. The superconductivity mediated by orbital fluctuations has a gap function of s_{++} -wave without sign reversal.^{3,4} Some experimental results such as ultrasonic measurement support the importance of the orbital degrees of freedom.^{5,6} In optimally K-doped BaFe_2As_2 , laser angle-resolved photoemission spectroscopy (ARPES) measurement provides results of the same magnitude of the superconducting gap on different hole FSs, which is difficult to explain by only the spin-fluctuation scenario.⁷ Moreover, a FS-selective gap structure including octet line nodes in the end member of the series KFe_2As_2 implies that several pairing mechanisms are competing, namely, spin and orbital fluctuations.⁸

To go forward with the identification of the pairing mechanism of IBSs, a phase-sensitive probe is required. The impurity effects have played a key role for this purpose since the study of cuprate superconductors.⁹ According to Anderson's theorem, nonmagnetic impurities do not work as a pair breaker in isotropic single-gap superconductors. By contrast, fast suppression of the superconducting transition temperature T_c is expected in superconductors with a sign change such as d wave, analogous to magnetic impurities in s -wave superconductors. In fact, this has been observed in cuprate superconductors, such as Zn-doped $\text{YBa}_2\text{Cu}_3\text{O}_{7-\delta}$ and $\text{Bi}_2\text{Sr}_2\text{CaCu}_2\text{O}_8$.⁹ In IBSs, pioneering studies have been reported.¹⁰⁻¹⁸ A peculiar way to introduce disorders is energetic particle irradiation. Defects created by 2.5-MeV electron irradiation are reported to behave similarly to Zn substitutions in $\text{YBa}_2\text{Cu}_3\text{O}_{7-\delta}$ (Ref. 19). In sharp contrast to chemical

substitution, light-particle irradiations enable us to systematically introduce pointlike defects in a given sample. The problems in chemical substitution, like structurally unstable and inhomogeneous properties and/or possible changes in carrier density and FS topology, can be also overcome. Such advantages are utilized to single crystalline IBSs to distinguish whether the gap has sign reversal or not. The most striking result obtained is in proton (H^+) irradiated $\text{Ba}(\text{Fe}_{1-x}\text{Co}_x)_2\text{As}_2$, which shows a depression of superconductivity slower than that expected for s_{\pm} -wave superconductors.¹⁵

Among several types of IBSs, BaFe_2As_2 is the prototypical system. Especially, optimally and over K-doped BaFe_2As_2 have very small residual resistivity (RR), so that the intrinsic impurity scattering is negligible.²⁰ This is in stark contrast to the Co-doped sample, where direct doping of Fe-site provides a large RR ($\sim 50 \mu\Omega \text{ cm}$ at optimal doping) even after BaAs annealing.^{20,21} Owing to the absence of the intrinsic scattering centers, we can safely attribute RR to extrinsically introduced scattering, which have a possibility of pair breaking.

In this paper, we report the suppression rate of T_c in underdoped, optimally doped, and overdoped $\text{Ba}_{1-x}\text{K}_x\text{Fe}_2\text{As}_2$ ($x = 0.23, 0.42, \text{ and } 0.69$) by 3-MeV proton (H^+) irradiation. The parallel shift without low-temperature upturn evidences the introduction of nonmagnetic impurity. The rate of T_c suppression is much weaker than that expected for s_{\pm} -wave superconductors, as in the case of Co-doped BaFe_2As_2 .

II. EXPERIMENTAL METHODS

Single crystals of underdoped and optimally K-doped BaFe_2As_2 were grown by FeAs self-flux method, whereas overdoped single crystals were synthesized by using other flux.²² The actual K-doping level was determined by energy dispersive x-ray spectroscopy. The resultant x of $\text{Ba}_{1-x}\text{K}_x\text{Fe}_2\text{As}_2$ was 0.23, 0.42, and 0.69 for underdoped, optimally doped, and overdoped crystals, respectively. All crystals were cleaved to be thin plates with thickness less than $\sim 25 \mu\text{m}$. This value is much smaller than the projected range of 3-MeV H^+ for $\text{Ba}_{1-x}\text{K}_x\text{Fe}_2\text{As}_2$ of $\sim 50 \mu\text{m}$, calculated by the stopping and range of ions in matter-2008.²³ Gold

wires were attached to the samples by silver paste with a standard four-probe configuration for *in situ* resistivity measurements. After they were loaded onto the sapphire plate, these crystals were cooled down by a closed-cycle refrigerator at the terminal of the irradiation port. The 3-MeV H^+ irradiation at $T = 50$ K was performed parallel to the c axis at NIRS-HIMAC. Since random point defects including Frenkel pairs, some of which are mobile even at room T (Ref. 24), are expected to be produced by 3-MeV H^+ irradiation,²⁵ we kept the temperature low (≤ 50 K) to stabilize defects during the following resistance measurements. The proton flux was limited to $\lesssim 10^{12}$ ions/cm²/s to avoid excessive heating of the crystals. The magneto-optical imaging was performed by using the local-field-dependent Faraday effect in the in-plane magnetized garnet indicator film employing a differential method.^{26,27}

III. RESULTS AND DISCUSSION

To ensure the quality of the samples, we have measured the resistivity (ρ) in a wide range of temperature (T). Figure 1 represents the result of ρ - T measurements in the as-grown samples, which are identical to those used in the irradiation study in the following. The absolute value of ρ at $T = 300$ K is slightly reduced with increasing x . Upon cooling, the crossover from high- T convex to low- T concave behavior is observed at the characteristic $T^* \simeq 100$ K. These results are quite consistent with the previous reports.^{20,28} In the low- T region $T \ll T^*$, a quadratic T dependence of ρ is observed in all three samples, which is obvious in the inset of Fig. 1. The superconducting transition occurs at $T_c = 24.4$ K, 37.4 K, and 17.8 K, in $x = 0.23$, 0.42, and 0.69, respectively, where T_c is defined by the midpoint of resistive transition. These values of T_c almost coincide with the onset of the Meissner signal measured by the superconducting quantum interference device magnetometer, which gives evidence for the bulk transition.

The central issue of this study is to clarify the relationship between the evolution of ρ_0 and the reduction of T_c , where ρ_0 is the residual resistivity. For this purpose, we have employed *in situ* resistance measurements right after the introduction of scattering centers. The ρ - T measurements after the H^+

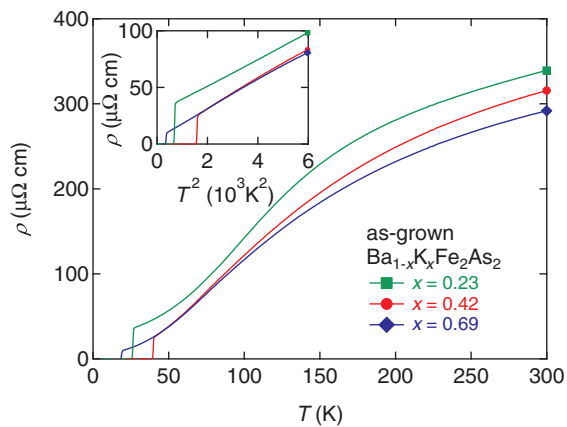


FIG. 1. (Color online) Temperature dependence of the resistivity in $Ba_{1-x}K_xFe_2As_2$ ($x = 0.23, 0.42,$ and 0.69). Inset: The resistivity as a function of T^2 .

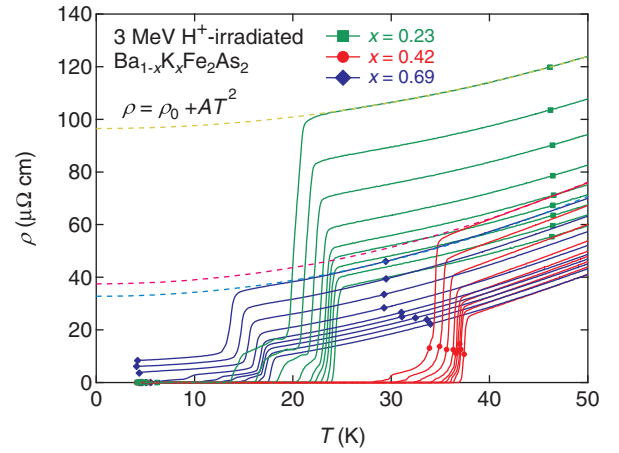


FIG. 2. (Color online) Temperature dependence of the resistivity in $Ba_{1-x}K_xFe_2As_2$ ($x = 0.23, 0.42,$ and 0.69) with doses of $0, 0.52, 1.0, 1.6, 2.1, 3.1, 4.8, 6.8,$ and 9.2×10^{16} ions/cm². Broken lines represent fitting lines of $\rho = \rho_0 + AT^2$.

irradiation up to a dose of 9.2×10^{16} ions/cm² are illustrated in Fig. 2. Regarding the normal state behavior, all samples show a parallel shift upon irradiation without any low- T upturn, indicating that the point defects introduced by this irradiation are nonmagnetic and no localization effects appear. This fact is quite important in view of the study of pair-breaking effects, since the stiffness of the superconductivity to the nonmagnetic scattering is the key to distinguish the possible sign-reversing order parameter. To estimate the impurity scattering rate, we have extrapolated ρ in the normal state to $T = 0$ K with a function of $\rho = \rho_0 + AT^2$ and calculated $\Delta\rho_0 \equiv \rho_0^i - \rho_0^0$, where ρ_0^i is ρ_0 of the i th irradiation. The evolutions of $\Delta\rho_0$ with the dose are depicted in Fig. 3(a). An almost linear increase in $\Delta\rho_0$ is evident in all samples, although the slope of the underdoped sample is twice as large as the slopes in the optimally doped and overdoped samples. On the other hand, we can see that T_c is gradually suppressed without significant broadening of the transition in all samples except for the tail part. We will come back to this point later. We define T_c by the midpoint of a sharp ρ drop, so that T_c as a function of the dose is shown in Fig. 3(b). Here the error bars are twice $T_c^{\text{onset}} - T_c$ (T_c^{onset} is the onset T of the ρ drop), which is smaller than ~ 1 K, except for underdoped sample at higher doses. T_c suppression, $\Delta T_c = T_{c0} - T_c$, is linear with a maximum reduction of 4.3, 3.0, and 4.3 K, for underdoped, optimally doped, and overdoped samples, respectively, where T_{c0} is T_c before the irradiation. It should be noted that this suppression of T_c is much larger than that reported for heavy-ion irradiated $(Ba,K)Fe_2As_2$ with a matching field of 21 T ($\Delta T_c \sim 0.3$ K), where the average spacing of columnar defects is 100 Å (Ref. 29).

Figure 4 represents T_c (main panel) and T_c/T_{c0} (inset) as a function of $\Delta\rho_0$. The suppression rates of T_c , $-\Delta T_c/\Delta\rho_0$, are 65 K/m Ω cm, 95 K/m Ω cm, and 161 K/m Ω cm for $x = 0.23, 0.42,$ and 0.69 , respectively. It is noteworthy that these values are comparable to the value of 46–77 K/m Ω cm in chemically substituted $Ba_{0.5}K_{0.5}Fe_2As_2$ (Ref. 17). The linear extrapolation, drawn by broken lines in Fig. 4, gives the critical residual resistivity value $\Delta\rho_0^{\text{cr}}$ to fully suppress T_c as 376,

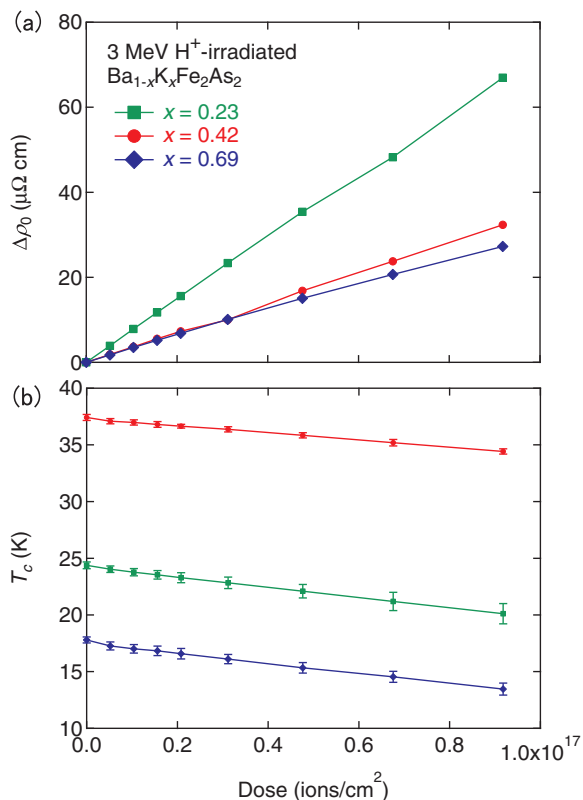


FIG. 3. (Color online) Dose dependence of (a) $\Delta\rho_0 \equiv \rho_0^i - \rho_0^0$ and (b) T_c in $\text{Ba}_{1-x}\text{K}_x\text{Fe}_2\text{As}_2$ ($x = 0.23, 0.42,$ and 0.69).

396, and 110 $\mu\Omega\text{ cm}$, respectively. These values of $\Delta\rho_0^{\text{cr}}$ for the underdoped and optimally doped samples are similar to previous reports (100–1000 $\mu\Omega\text{ cm}$)^{14–17} and consistent with theoretical study.³ The overdoped sample, on the other hand, has a smaller $\Delta\rho_0^{\text{cr}}$. The fast suppression rate of T_c in the overdoped sample can be seen even in the T_c/T_{c0} vs $\Delta\rho_0$, depicted in the inset of Fig. 4. The slope in the overdoped

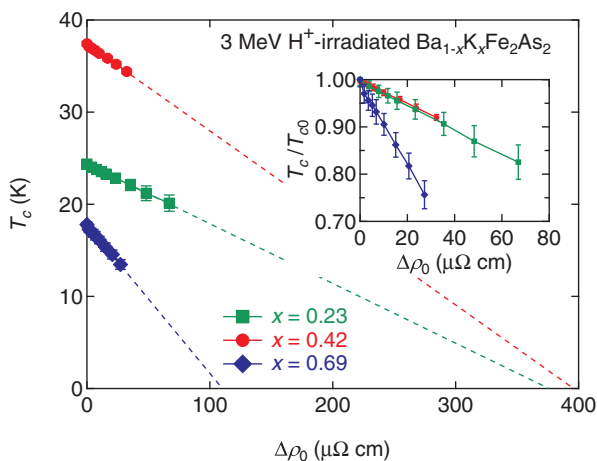


FIG. 4. (Color online) T_c as a function of $\Delta\rho_0$ in $\text{Ba}_{1-x}\text{K}_x\text{Fe}_2\text{As}_2$ ($x = 0.23, 0.42,$ and 0.69). Inset: The vertical axis is changed to T_c/T_{c0} .

sample is 3.5 times larger than the slopes of the underdoped and optimally doped samples.

For quantitative discussion of pair-breaking effects by non-magnetic scatterings, we evaluate the normalized scattering rate $g = \hbar/2\pi k_B T_{c0} \tau$, where \hbar , k_B , and τ are the Planck's constant divided by 2π , the Boltzmann constant, and the scattering time, respectively. If we assume the intraband scattering rate τ_{intra}^{-1} and the interband scattering rate τ_{inter}^{-1} are the same, i.e., $\tau_{\text{intra}}^{-1} \simeq \tau_{\text{inter}}^{-1} \equiv \tau^{-1}$, then $1/\Delta\rho_0 = 1/\Delta\rho_{\text{intra}} + 1/\Delta\rho_{\text{inter}} = (ne^2/m^*)(\tau_{\text{intra}} + \tau_{\text{inter}}) = 2ne^2/m^* \tau^{-1}$, and we can estimate τ^{-1} from $\Delta\rho_0$ as $\tau^{-1} = 2ne^2 \Delta\rho_0/m^*$, where n is the carrier density, e is the elementary charge, and m^* is the effective quasiparticle mass. In the following, we show three different estimations of g : g^{5orb} , g^λ , and g^H , which are described in Figs. 5(a), 5(b), and 5(c), respectively.

According to linear response theory based on the five-orbital model, we obtain the relation $\Delta\rho_0$ ($\mu\Omega\text{ cm}$) = $0.18\tau^{-1}$ (K) in $\text{Ba}_{1-x}\text{K}_x\text{Fe}_2\text{As}_2$, leading to the first estimation of $g^{\text{5orb}} = 0.88z \Delta\rho_0/T_{c0}$, where z is the renormalization factor.³⁰ The angle-resolved photoemission spectroscopy measurement in $\text{Ba}_{0.6}\text{K}_{0.4}\text{Fe}_2\text{As}_2$ gives a result of the renormalization factor $z = 1/2$ (Refs. 31 and 32). The obtained T_c/T_{c0} as a function of g^{5orb} is shown in Fig. 5(a). The critical values of g ($\equiv g_c$) where the linear extrapolation of T_c/T_{c0} goes to zero are evaluated as 6.8, 4.7, and 2.7 in $x = 0.23, 0.42,$ and 0.69 , respectively. These values compare well with those obtained for substitutions of Mn, Co, Ni, Cu, and Zn for Fe in almost optimally doped crystals of $\text{Ba}_{0.5}\text{K}_{0.5}\text{Fe}_2\text{As}_2$, $g_c = 4-8$.¹⁷

With London penetration depth $\lambda = \sqrt{m^*/\mu_0 n e^2}$, we can obtain another estimation of τ^{-1} as $\tau^{-1} = ne^2 \Delta\rho_0/m^* = \Delta\rho_0/\mu_0 \lambda^2$, where μ_0 is the vacuum permeability. It is noted that the use of λ allows us to avoid direct estimation of n and m^* . Optical measurements in the low-frequency limit give $\lambda \simeq 2000\text{ \AA}$ in $\text{Ba}_{0.6}\text{K}_{0.4}\text{Fe}_2\text{As}_2$ (Ref. 33). Without considering the K doping dependence of λ , we obtain the second estimation $g^\lambda = \hbar \Delta\rho_0/\pi k_B T_{c0} \mu_0 \lambda^2$. T_c/T_{c0} as a function of g^λ is shown in Fig. 5(b). The critical values g_c of the normalized scattering rate obtained from linear extrapolations are 7.5, 5.1, and 3.0 in $x = 0.23, 0.42,$ and 0.69 , respectively.

The conventional approach to estimate carrier density n is from Hall coefficient R_H measurements. R_H at 300 K is reported to be $\sim 1 \times 10^{-9} \text{ m}^3/\text{C}$ (Refs. 28,34, and 35), which offers the third estimation of $g^H = \hbar \Delta\rho_0 e/\pi k_B T_{c0} m^* R_H$. With the mass enhancement factor $m^* = 2m$ as mentioned above, the critical scattering rates g_c for $x = 0.23, 0.42,$ and 0.69 are estimated as $g_c = 33, 23,$ and 13 , respectively. Here m is assumed to be the free electron mass. These values are more than 4 times larger than the other estimations above. This is possibly because R_H is not a good measure of n in $\text{Ba}_{1-x}\text{K}_x\text{Fe}_2\text{As}_2$, since the T variation of R_H is ascribed to several contributions such as multiband nature, antiferromagnetic spin fluctuations, Fermi surface reconstruction, and so on. Unfortunately, it is difficult to separate these contributions from others. For example, Ohgushi and Kiuchi analyzed R_H in $\text{Ba}_{1-x}\text{K}_x\text{Fe}_2\text{As}_2$ assuming a two-band model with an expression of hole carrier density $n_h = n_0 + \frac{x}{2} \frac{m_h}{m_h + m_e}$ and electron carrier density $n_e = n_0 - \frac{x}{2} \frac{m_e}{m_h + m_e}$ and found a strong T dependence of n_0 and m_h/m_e (Ref. 28). This means that the estimation of g^H largely depends on the choice of T in

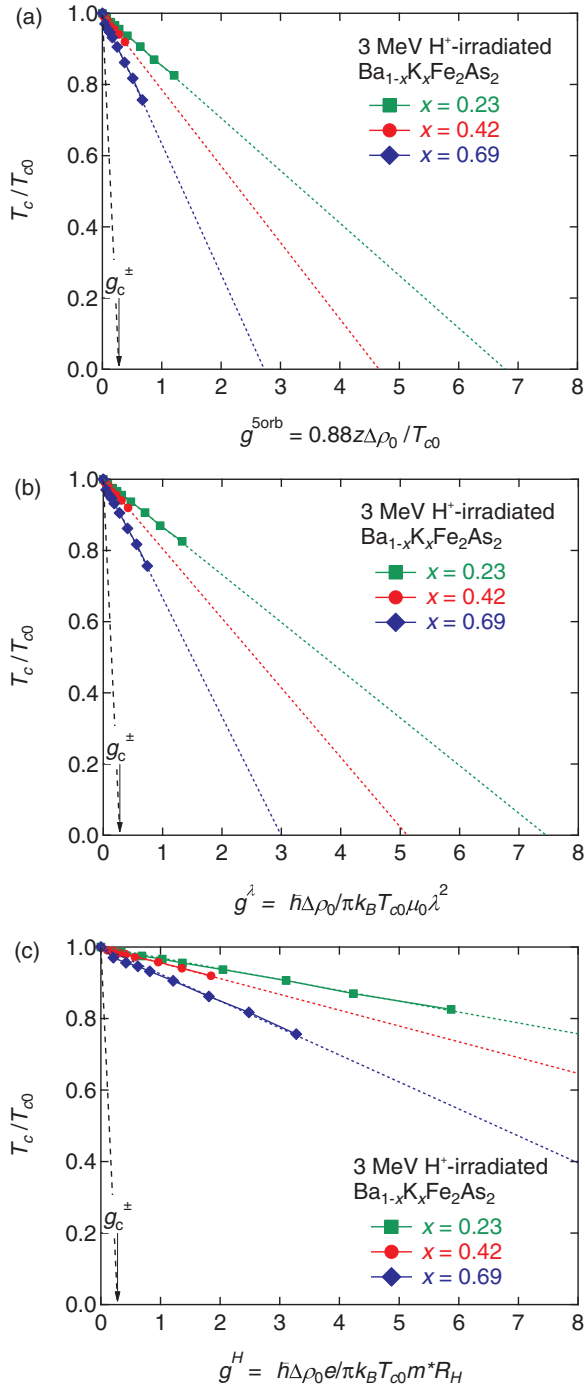


FIG. 5. (Color online) T_c/T_{c0} as a function of a normalized scattering rate $g = \hbar/2\pi k_B T_{c0} \tau$ in $\text{Ba}_{1-x}\text{K}_x\text{Fe}_2\text{As}_2$ ($x = 0.23, 0.42$, and 0.69) evaluated by (a) the five-orbital model $g^{5\text{orb}} = 0.88z\Delta\rho_0/T_{c0}$, (b) the London penetration depth $g^\lambda = \hbar\Delta\rho_0/\pi k_B T_{c0} \mu_0 \lambda^2$, and (c) the Hall coefficient $g^H = \hbar\Delta\rho_0 e / \pi k_B T_{c0} m^* R_H$. These data are linearly extrapolated to obtain critical values of g as shown by dotted lines. Dashed lines indicate the critical scattering rate $g_c^\pm \simeq 0.3$ by simple estimation for the s_\pm -wave scenario.

R_H . In addition, we cannot use R_H at low T since an apparent spin-fluctuation effect is identified as evidenced by a strong T dependence of R_H , especially in underdoped samples. Thus g^H must overestimate the scattering rate.

These three results should be compared with the s_\pm -wave scenario with equal gap magnitudes of opposite signs on different FSs. Provided the simplest assumption of $\tau_{\text{intra}}^{-1} = \tau_{\text{inter}}^{-1}$, the pair breaking is evaluated by the Abrikosov-Gor'kov formula, $-\ln T_c/T_{c0} = \psi(1/2 + gT_{c0}/2T_c) - \psi(1/2)$, where $\psi(x)$ is a digamma function and $g = \hbar\tau_{\text{inter}}^{-1}/2\pi k_B T_{c0}$. The obtained critical g in this scenario is $g_c^\pm \simeq 0.3$, as shown in Figs. 5(a)–5(c). Obviously, all estimates of g_c are much larger than $g_c^\pm \simeq 0.3$. By contrast, it is expected that the rate of T_c suppression is much smaller in the s_{++} -wave scenario. Therefore, our results strongly suggest that the realization of the s_\pm -wave gap function in K-doped BaFe_2As_2 is unlikely. However, it should be noted that an impurity-robust s_\pm state has recently been discussed by changing the ratio of inter- to intraband scatterings.^{36,37} To examine if the anomalously small ratio of inter- to intraband scattering is feasible, Yamakawa *et al.*³⁸ have recently studied the nonlocal impurity scattering effect in accordance with the first-principle study deriving $3d$ - and $4d$ -impurity potentials.³⁹ They have found that the negligible interband scattering is unrealistic and $-\Delta T_c/\Delta\rho_0$ is independent of the impurity potential strength and T_{c0} . They concluded that the s_\pm -wave state is inconsistent with the experimental results reported in IBSSs, which is consistent with the local impurity model in Ref. 4. The results obtained in Refs. 3, 36, 37, and 40–44 are based on orbital-less multiband model. In this model, the amplitude of interband scattering becomes negligible in a unitary impurity scattering regime. This is why a wide range of ratios of intra- to interband scatterings is examined, and at a small interband scattering rate the superconductivity is robust even in the s_\pm -wave state. However, this model neglects the momentum dependence of the impurity potential originated from the orbital degrees of freedom. When taking it into account, i.e., based on the five-orbital model, it is revealed that a large interband scattering should appear and the s_\pm state is fragile. Hence, we must adopt the comparable interband scattering to the intraband one. Although we cannot specify the ratio of inter- to intraband scattering rates, the ratio is not completely an arbitrary assumption. Our present results manifest the robustness of T_c against the introduction of impurity scatterings, and based on the above consideration, we can safely conclude that they are inconsistent with the s_\pm -wave state in the $\text{Ba}_{1-x}\text{K}_x\text{Fe}_2\text{As}_2$ system. We should additionally point out that faster suppression of T_c/T_{c0} in highly overdoped samples is possibly realized if the mass enhancement m^*/m is large, taking the stronger correlation in the end member of KFe_2As_2 into account.^{45,46} The disappearance of the electron FS sheets and the negligible gap size of the outer hole FS are reported for $x \geq 0.6$, leading to possible crossover of the superconducting order parameter, caused by the competition between the pairing mechanisms, probably the orbital fluctuation and the spin fluctuation.^{47,48} The observed faster suppression of T_c/T_{c0} in the $x = 0.69$ sample might be related to such differences.

Here we stress the advantage of K-doped BaFe_2As_2 to discuss impurity effects. As already mentioned above, the as-grown K-doped system has no intrinsic impurity scattering, i.e., negligible RR, so we can discuss all the above by means of ρ_0 instead of $\Delta\rho_0$. This enables us to make a straightforward transformation from the RR to the impurity scattering rate.

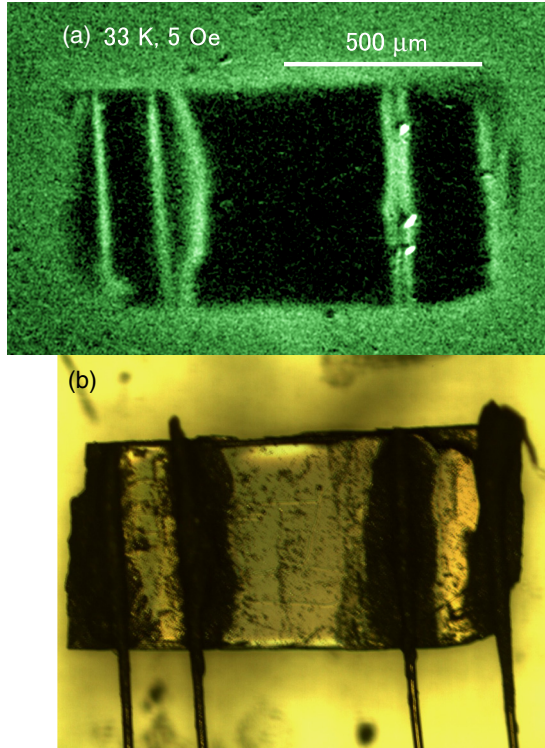


FIG. 6. (Color online) (a) A magneto-optical image at 33 K under $H = 5$ Oe taken after removing silver paste and gold wire from the crystal of $\text{Ba}_{0.6}\text{K}_{0.4}\text{Fe}_2\text{As}_2$ shown in panel (b).

Even if we do so, the obtained results are almost the same because of very small ρ_0^0 . This point gives a significant advantage compared with the Co-doped system, where we can understand the origin of the increment $\Delta\rho_0$ only but not clearly of ρ_0^0 . Once we are able to obtain high-quality single crystals of K-doped BaFe_2As_2 , the study in this sample is more suitable than that in the Co-doped one to purely testify to the robustness of superconductivity against impurity scattering.

Finally, we comment on the tail of resistive transition. Namely, by increasing the irradiation dose, a finite value of ρ remains after the main superconducting transition followed by the second broad transition at a low T . To clarify the origin, we performed magneto-optical (MO) imaging in a similar crystal of H^+ -irradiated $\text{Ba}_{0.6}\text{K}_{0.4}\text{Fe}_2\text{As}_2$ [Fig. 6(b)] after carefully removing silver paste and gold wires. Figure 6(a) shows an example of the MO image at $T = 33$ K under $H = 5$ Oe. Under this low-field condition, the superconducting region gives a Meissner response, which shows up as a dark part

in the MO image. This is actually observed in most parts of the crystal. Additional dark regions are detected at the very narrow regions just beneath gold wires, surrounded by bright regions, where the superconductivity is weakened or lost. This positional-dependent magnetic response addresses lower T_c beneath the silver paste. One of the possible origins for such a stronger suppression of T_c is that lower-energy H^+ ions and/or the secondary electrons generated in the silver paste are more effective in introducing point defects. Hence we conclude that the fast suppression of superconductivity under silver paste accompanied by the spatially modulated T_c is the origin of the tail in resistive transition. A close inspection of the ρ - T data in Fig. 2 allows us to roughly estimate $(T_{c0} - T_c^{\rho=0})/\Delta T_c \sim 2$ in $x = 0.23$ and 0.42 , while ~ 3 in $x = 0.69$. Since ΔT_c is proportional to $\Delta\rho_0$, ρ_0 of the part beneath the silver paste is estimated to be twice as large as that of the bare part in $x = 0.23$ and 0.42 , while it is 3 times as large in $x = 0.69$. Here the main transition at T_c is attributed to the property of the bare parts and zero resistivity appears at $T_c^{\rho=0}$ as a consequence of transition in the region beneath the silver paste. Since the volume beneath the silver paste is much smaller than that of the bare parts, the serial circuit of these parts provides only a small correction to ρ_0 . Such a few percent enhancement of the RR does not affect the pair-breaking discussion above.

IV. SUMMARY

We have evaluated the impurity effects in underdoped, optimally doped, and overdoped $\text{Ba}_{1-x}\text{K}_x\text{Fe}_2\text{As}_2$ single crystals by means of 3-MeV H^+ irradiation. All samples show a parallel shift of the ρ - T curves by the irradiation, which manifests that defects introduced by the irradiation are nonmagnetic and are not causing localization effects. Almost linear variations of $\Delta\rho_0$ and T_c as a function of dose are obtained. The critical value of the normalized scattering rate g_c is estimated by three different methods. By assuming a realistic condition of similar magnitudes of intra- and interband scattering rates, all obtained g_c 's are much larger than g_c^\pm , inconsistent with the s_{\pm} -wave state in $\text{Ba}_{1-x}\text{K}_x\text{Fe}_2\text{As}_2$.

ACKNOWLEDGMENTS

We would like to acknowledge S. Ishida for advice on the sample synthesis and H. Kontani for fruitful discussions. This work is partly supported by a Grant-in-Aid for JSPS Fellows and a grant-in-aid from MEXT in Japan and is part of the Research Project with Heavy Ions at NIRS-HIMAC.

*toshihiro.taen@09.alumni.u-tokyo.ac.jp

¹K. Kuroki, S. Onari, R. Arita, H. Usui, Y. Tanaka, H. Kontani, and H. Aoki, *Phys. Rev. Lett.* **101**, 087004 (2008).

²I. I. Mazin, D. J. Singh, M. D. Johannes, and M. H. Du, *Phys. Rev. Lett.* **101**, 057003 (2008).

³S. Onari and H. Kontani, *Phys. Rev. Lett.* **103**, 177001 (2009).

⁴H. Kontani and S. Onari, *Phys. Rev. Lett.* **104**, 157001 (2010).

⁵T. Goto, R. Kurihara, K. Araki, K. Mitsumoto, M. Akatsu, Y. Nemoto, S. Tatematsu, and M. Sato, *J. Phys. Soc. Jpn.* **80**, 073702 (2011).

⁶M. Yoshizawa, D. Kimura, T. Chiba, S. Simayi, Y. Nakanishi, K. Kihou, C.-H. Lee, A. Iyo, H. Eisaki, M. Nakajima, and S. ichi Uchida, *J. Phys. Soc. Jpn.* **81**, 024604 (2012).

⁷T. Shimojima, F. Sakaguchi, K. Ishizaka, Y. Ishida, T. Kiss, M. Okawa, T. Togashi, C.-T. Chen, S. Watanabe, M. Arita, K. Shimada, H. Namatame, M. Taniguchi, K. Ohgushi, S. Kasahara, T. Terashima, T. Shibauchi, Y. Matsuda, A. Chainani, and S. Shin, *Science* **332**, 564 (2011).

⁸K. Okazaki, Y. Ota, Y. Kotani, W. Malaeb, Y. Ishida, T. Shimojima, T. Kiss, S. Watanabe, C.-T. Chen, K. Kihou, C. H. Lee, A. Iyo,

- H. Eisaki, T. Saito, H. Fukazawa, Y. Kohori, K. Hashimoto, T. Shibauchi, Y. Matsuda, H. Ikeda, H. Miyahara, R. Arita, A. Chainani, and S. Shin, *Science* **337**, 1314 (2012).
- ⁹H. Alloul, J. Bobroff, M. Gabay, and P. J. Hirschfeld, *Rev. Mod. Phys.* **81**, 45 (2009).
- ¹⁰A. Kawabata, S. C. Lee, T. Moyoshi, Y. Kobayashi, and M. Sato, *J. Phys. Soc. Jpn.* **77**, 103704 (2008).
- ¹¹A. E. Karkin, J. Werner, G. Behr, and B. N. Goshchitskii, *Phys. Rev. B* **80**, 174512 (2009).
- ¹²M. Sato, Y. Kobayashi, S. C. Lee, H. Takahashi, E. Satomi, and Y. Miura, *J. Phys. Soc. Jpn.* **79**, 014710 (2010).
- ¹³S. C. Lee, E. Satomi, Y. Kobayashi, and M. Sato, *J. Phys. Soc. Jpn.* **79**, 023702 (2010).
- ¹⁴C. Tarantini, M. Putti, A. Gurevich, Y. Shen, R. K. Singh, J. M. Rowell, N. Newman, D. C. Larbalestier, P. Cheng, Y. Jia, and H.-H. Wen, *Phys. Rev. Lett.* **104**, 087002 (2010).
- ¹⁵Y. Nakajima, T. Taen, Y. Tsuchiya, T. Tamegai, H. Kitamura, and T. Murakami, *Phys. Rev. B* **82**, 220504 (2010).
- ¹⁶J. Li, Y. Guo, S. Zhang, S. Yu, Y. Tsujimoto, H. Kontani, K. Yamaura, and E. Takayama-Muromachi, *Phys. Rev. B* **84**, 020513 (2011).
- ¹⁷J. Li, Y. F. Guo, S. B. Zhang, J. Yuan, Y. Tsujimoto, X. Wang, C. I. Sathish, Y. Sun, S. Yu, W. Yi, K. Yamaura, E. Takayama-Muromachi, Y. Shirako, M. Akaogi, and H. Kontani, *Phys. Rev. B* **85**, 214509 (2012).
- ¹⁸K. Kirshenbaum, S. R. Saha, S. Ziemak, T. Drye, and J. Paglione, *Phys. Rev. B* **86**, 140505 (2012).
- ¹⁹F. Rullier-Albenque, P. A. Vieillefond, H. Alloul, A. W. Tyler, P. Lejay, and J. F. Marucco, *Europhys. Lett.* **50**, 81 (2000).
- ²⁰S. Ishida, M. Nakajima, T. Liang, K. Kihou, C.-H. Lee, A. Iyo, H. Eisaki, T. Kakeshita, Y. Tomioka, T. Ito, and S.-I. Uchida, *J. Am. Chem. Soc.* **135**, 3158 (2013).
- ²¹Y. Nakajima, T. Taen, and T. Tamegai, *J. Phys. Soc. Jpn.* **78**, 023702 (2009).
- ²²K. Kihou *et al.* (unpublished).
- ²³J. Ziegler, J. Biersack, and U. Littmark, *The Stopping and Range of Ions in Solids* (Pergamon, New York, 1985), p. 202.
- ²⁴A. D. Marwick, G. J. Clark, D. S. Yee, R. B. Laibowitz, G. Coleman, and J. J. Cuomo, *Phys. Rev. B* **39**, 9061 (1989), and references therein.
- ²⁵N. Haberkorn, B. Maiorov, I. O. Usov, M. Weigand, W. Hirata, S. Miyasaka, S. Tajima, N. Chikumoto, K. Tanabe, and L. Civale, *Phys. Rev. B* **85**, 014522 (2012).
- ²⁶A. Soibel, E. Zeldov, M. Rappaport, Y. Myasoedov, T. Tamegai, S. Ooi, M. Konczykowski, and V. B. Geshkenbein, *Nature (London)* **406**, 282 (2000).
- ²⁷M. Yasugaki, K. Itaka, M. Tokunaga, N. Kameda, and T. Tamegai, *Phys. Rev. B* **65**, 212502 (2002).
- ²⁸K. Ohgushi and Y. Kiuchi, *Phys. Rev. B* **85**, 064522 (2012).
- ²⁹L. Fang, Y. Jia, C. Chaparro, G. Sheet, H. Claus, M. A. Kirk, A. E. Koshelev, U. Welp, G. W. Crabtree, W. K. Kwok, S. Zhu, H. F. Hu, J. M. Zuo, H.-H. Wen, and B. Shen, *Appl. Phys. Lett.* **101**, 012601 (2012).
- ³⁰H. Kontani and M. Sato, [arXiv:1005.0942](https://arxiv.org/abs/1005.0942).
- ³¹D. V. Evtushinsky, D. S. Inosov, V. B. Zabolotnyy, M. S. Viazovska, R. Khasanov, A. Amato, H.-H. Klauss, H. Luetkens, C. Niedermayer, G. L. Sun, V. Hinkov, C. T. Lin, A. Varykhalov, A. Koitzsch, M. Knupfer, B. Büchner, A. A. Kordyuk, and S. V. Borisenko, *New J. Phys.* **11**, 055069 (2009).
- ³²H. Ding, K. Nakayama, P. Richard, S. Souma, T. Sato, T. Takahashi, M. Neupane, Y.-M. Xu, Z.-H. Pan, A. V. Fedorov, Z. Wang, X. Dai, Z. Fang, G. F. Chen, J. L. Luo, and N. L. Wang, *J. Phys.: Condens. Matter* **23**, 135701 (2011).
- ³³G. Li, W. Z. Hu, J. Dong, Z. Li, P. Zheng, G. F. Chen, J. L. Luo, and N. L. Wang, *Phys. Rev. Lett.* **101**, 107004 (2008).
- ³⁴B. Shen, H. Yang, Z.-S. Wang, F. Han, B. Zeng, L. Shan, C. Ren, and H.-H. Wen, *Phys. Rev. B* **84**, 184512 (2011).
- ³⁵D. V. Evtushinsky, A. A. Kordyuk, V. B. Zabolotnyy, D. S. Inosov, T. K. Kim, B. Büchner, H. Luo, Z. Wang, H.-H. Wen, G. Sun, C. Lin, and S. V. Borisenko, *J. Phys. Soc. Jpn.* **80**, 023710 (2011).
- ³⁶D. V. Efremov, M. M. Korshunov, O. V. Dolgov, A. A. Golubov, and P. J. Hirschfeld, *Phys. Rev. B* **84**, 180512 (2011).
- ³⁷Y. Wang, A. Kreisler, P. J. Hirschfeld, and V. Mishra, *Phys. Rev. B* **87**, 094504 (2013).
- ³⁸Y. Yamakawa, S. Onari, and H. Kontani, *Phys. Rev. B* **87**, 195121 (2013).
- ³⁹K. Nakamura, R. Arita, and H. Ikeda, *Phys. Rev. B* **83**, 144512 (2011).
- ⁴⁰A. V. Chubukov, D. V. Efremov, and I. Eremin, *Phys. Rev. B* **78**, 134512 (2008).
- ⁴¹Y. Senga and H. Kontani, *J. Phys. Soc. Jpn.* **77**, 113710 (2008).
- ⁴²Y. Bang, H.-Y. Choi, and H. Won, *Phys. Rev. B* **79**, 054529 (2009).
- ⁴³Y. Senga and H. Kontani, *New J. Phys.* **11**, 035005 (2009).
- ⁴⁴Z.-J. Yao, W.-Q. Chen, Y.-K. Li, G.-H. Cao, H.-M. Jiang, Q.-E. Wang, Z.-A. Xu, and F.-C. Zhang, *Phys. Rev. B* **86**, 184515 (2012).
- ⁴⁵T. Terashima, N. Kurita, M. Kimata, M. Tomita, S. Tsuchiya, M. Imai, A. Sato, K. Kihou, C.-H. Lee, H. Kito, H. Eisaki, A. Iyo, T. Saito, H. Fukazawa, Y. Kohori, H. Harima, and S. Uji, *Phys. Rev. B* **87**, 224512 (2013).
- ⁴⁶H. Ikeda, R. Arita, and J. Kuneš, *Phys. Rev. B* **82**, 024508 (2010).
- ⁴⁷W. Malaeb, T. Shimojima, Y. Ishida, K. Okazaki, Y. Ota, K. Ohgushi, K. Kihou, T. Saito, C. H. Lee, S. Ishida, M. Nakajima, S. Uchida, H. Fukazawa, Y. Kohori, A. Iyo, H. Eisaki, C.-T. Chen, S. Watanabe, H. Ikeda, and S. Shin, *Phys. Rev. B* **86**, 165117 (2012).
- ⁴⁸D. Watanabe, T. Yamashita, Y. Kawamoto, S. Kurata, Y. Mizukami, T. Ohta, S. Kasahara, M. Yamashita, T. Saito, H. Fukazawa, Y. Kohori, S. Ishida, K. Kihou, C. H. Lee, A. Iyo, H. Eisaki, A. B. Vorontsov, T. Shibauchi, and Y. Matsuda, [arXiv:1307.3408](https://arxiv.org/abs/1307.3408).